2022-08-15

Air Quality Impacts from Mineral Dust, Fireworks, and Urban Pollution Revealed by Trace Element Chemistry and Strontium Isotopes Ratios in the Wasatch Front, Utah, USA

Micah J. Marcy
Brigham Young University

Air Quality Impacts from Mineral Dust, Fireworks, and Urban Pollution Revealed by Trace Element Chemistry and Strontium Isotope Ratios in the Wasatch Front, Utah, USA

Micah J. Marcy

A thesis submitted to the faculty of
Brigham Young University
in partial fulfillment of the requirements for the degree of

Master of Science

Gregory T. Carling, Chair
Barry R. Bickmore
Stephen T. Nelson

Department of Geological Sciences

Brigham Young University

ABSTRACT

Air Quality Impacts from Mineral Dust, Fireworks, and Urban Pollution Revealed by Trace Element Chemistry and Strontium Isotope Ratios in the Wasatch Front, Utah, USA

Micah J. Marcy
Department of Geological Sciences, BYU
Master of Science

Airborne particulate matter (PM) in urban areas is derived from a combination of natural and anthropogenic sources. To identify PM sources and their effects on air quality, we collected PM using active filter samplers over a two-year period in the urban Wasatch Front, northern Utah, an area affected by multiple pollution sources. Filters from active samplers and other PM samples were analyzed for major and trace element concentrations and $^{87}Sr/^{86}Sr$ ratios. We identified wind-blown mineral dust from dry lake beds, winter inversions, and fireworks as primary PM sources affecting air quality in the Wasatch Front. Dust contributes Al, Be, Ca, Co, Cs, Fe, Li, Mg, Mn, Rb, Th, U, Y, and REEs which are typical components of carbonate and silicate minerals. Winter inversions entrap As, Cd, Mo, Pb, Sb, Tl, and Zn from brake dust, combustion engine exhaust, and refining processes. Concentrations of common components of fireworks Ba, Cu, K, and Sr greatly increase (>4 times) during holidays. Strontium released from fireworks has a distinct $^{87}Sr/^{86}Sr$ ratio that dominates the isotopic composition of PM during holidays. Fireworks have $^{87}Sr/^{86}Sr$ ratios of <0.7080 compared with 0.7100 for Sevier Dry Lake and 0.7150 for Great Salt Lake lakebed. Sources of particulate matter vary seasonally. Dust events dominate the air quality signature during spring and summer while winter inversions occur from November through February. Transport of PM to mountain snowpack negatively affect water quality. This is the first study to describe variations in multiple PM sources and their potential health effects in Utah, USA.

Keywords: dust, fireworks, inversions, air quality, strontium isotopes, trace elements, particulate matter, Wasatch Front

ACKNOWLEDGEMENTS

I would like to thank my advisor Dr. Greg Carling for his assistance throughout each step of my thesis. I would also like to thank Dr. Barry Bickmore and Dr. Steve Nelson for their insights and suggestions. A special thanks to Alyssa Pope for managing the MiniVol samplers for two years and Dr. Diego Fernandez at the University of Utah for help with various lab results. Thank you to the Utah Department of Air Quality for the Science for Solutions Grant that funded this work. Above all, thank you to my wife Tess for supporting me and pushing me to put forward my best work.

TABLE OF CONTENTS

LIST OF TABLES

LIST OF FIGURES

1. Introduction

Air quality in urban areas is affected by a mixture of airborne particulate matter (PM) from natural and urban sources, but it is often difficult to identify these sources. Urban sources of PM include refining processes (Kulkarni et al., 2007), combustion, vehicle exhaust, and tire and brake abrasion (Karagulian et al., 2015; Tao et al., 2009; Wang et al., 2000). Particulate matter is also emitted by human activity at construction sites, gravel pits, and mines (Belnap and Gillette, 1998; He et al., 2007; Karagulian et al., 2015; Kulkarni et al., 2007; Wang et al., 2000). Natural sources of PM include wildfire smoke, and windblown mineral dust from burned areas and desert regions (Goudie, 2009; Hahnenberger and Nicoll, 2012). Particulate matter is divided by particle size. Particulate matter smaller than 2.5 microns is labeled $PM_{2.5}$, material smaller than 10 microns is labeled PM_{10}, and the total suspended particulate load is called TSP.

Regions with elevated levels of PM, especially $PM_{2.5}$, are linked to increased cases of asthma, pneumonia, and valley fever in local populations (Goudie, 2014; Pope et al., 1990; Pope et al., 1999). Dust is also linked to harmful algal blooms (Zhang, 1994), early snowmelt, and decreased mountain snowpack runoff (Painter et al., 2007; Painter et al., 2010). Tracking dust between source locations and impacted areas is necessary to determine future land use and water diversions that could alter dust regimes and affect downwind populations.

In the western United States, PM from desert regions including playas (i.e., mineral dust) is regularly transported during dust events to urban populations. These dust events are becoming more frequent because of the decline of saline lakes, over grazing, mining, and other anthropogenic activities (Goudie, 2009; Prospero, 2002; Skiles et al., 2018; Steenburgh et al., 2012; Wurtsbaugh et al., 2017). The desiccation of saline lakes around the globe is exposing large areas of unconsolidated lakebed sediments that are, in some cases, rich in chemical runoff

and heavy metals from agriculture and industrial complexes (Indoitu et al., 2015; Micklin, 2010). Unconsolidated sediments from Owens Dry Lake in California and the Great Salt Lake in Utah are regularly transported to neighboring metropolitan areas (Carling et al., 2020; Goudie, 2009; Neff et al., 2008; Prospero, 2002; Reynolds et al., 2007; Skiles et al., 2018; Steenburgh et al., 2012; Wurtsbaugh et al., 2017). During the last century PM from natural sources has increased 500% because of human activity (Neff et al., 2008).

Inversions are meteorological phenomenon where cold becomes trapped in valleys below a warm layer of air. This stagnated air forms a layer of persistent fog that becomes increasingly concentrated in anthropogenic pollutants that degrade the air quality the longer the inversion continues (Gillies et al., 2010; Whiteman et al., 1999; Wolyn and McKee, 1989b). Winter inversion often elevate $PM_{2.5}$ levels above the 24-hour National Ambient Air Quality Standard (NAAQS) of 35 $\mu g/m^3$ (Simon Wang et al., 2015).

Many festivals and celebrations around the world involve the use of fireworks including New Year's Eve (Worldwide), Lunar New Year (China), Diwali (India), Guy Fawkes Night (UK), and the Independence Day (USA). Smoke from fireworks is an important short-term source of anthropogenic pollutants that impacts local air quality (Singh et al., 2019), water quality (Wilkin et al., 2007), and snowpack (Steinhauser et al., 2008). The elements Ba, Sr, Mg, K, and Cu have been used as tracers of firework PM to better understand the effect of fireworks on air quality (Singh et al., 2019; Vecchi et al., 2008).

Geochemistry has been used to create "fingerprints" for different PM sources to identify the impacts on air quality. Fingerprinting is the process of identifying unique geochemical properties to distinguish PM sources from each other. Geochemistry and fingerprinting have been used extensively in tracking PM from dry lake beds and playas (Aarons et al., 2017; Beavington and

Cawse, 1979; Belnap and Gillette, 1998; Carling et al., 2012; Carling et al., 2020; Goodman et al., 2019; Goudie, 2009; Grousset and Biscaye, 2005), the role of fireworks on air quality (Singh et al., 2019; Steinhauser et al., 2008; Vecchi et al., 2008), and urban pollution source identification (Moreno et al., 2010; Sudheer and Rengarajan, 2012). A sequential acid leach process is used to separate fractions of elements that dynamically interact with the environment (bioavailable fraction) from elements with limited reactivity in the environment (immobile fraction) (Lanno et al., 2004). Sr isotope ratios ($^{87}Sr/^{86}Sr$) have been used to differentiate mineral sources which include playas, alluvial fans, and sand dunes (Aarons et al., 2017; Carling et al., 2020; Dastrup et al., 2018; Munroe et al., 2019; Nicoll et al., 2020). However, $^{87}Sr/^{86}Sr$ ratios have not been applied to distinguish natural and anthropogenic PM from each other.

When mineral dust mixes with urban PM the resulting mixture is enriched in trace and heavy metals (Sudheer and Rengarajan, 2012). To detangle mineral and urban dust for source apportionment, a variety of methods are employed including Positive Matrix Factorization (PMF) and Principal Component Analysis (PCA). PMF is a bilinear multivariate receptor that can identify PM factor contributions and factor profiles. A factor is a source with a unique signature that is identifiable by PMF (Beuck et al., 2011; Brown et al., 2015; Lee et al., 1999; Nicolás et al., 2008; Sudheer and Rengarajan, 2012). PCA is a method for reorienting the axes of a multivariate date set through rotation to describe the maximum amount of variation with the fewest possible dimensions (Miller-Schulze et al., 2015).

The purpose of our study is to track trace element chemistry and strontium isotopes in PM in an urban area impacted by mineral dust to evaluate air quality impacts of multiple sources. Specific objectives are to: 1) demonstrate the effects of different pollution sources (e.g., inversions, fireworks, dust events) on air quality; 2) use Sr isotopes to track dust events and

identify sources for specific events; 3) use PCA and PMF to create a geochemical fingerprint of different PM sources; and 4) quantify relative amount of metals in the readily leachable or bioavailable fraction. Our study was conducted in the Wasatch Front in northern Utah, an urban area with poor air quality that is impacted by dust events, winter inversions, wildfire smoke, firework smoke, and fugitive dust from mining, oil, and gas production.

2. Study Area

The Wasatch Front is a metropolitan area adjacent to the Wasatch Range in northern Utah that is home to more than 2.5 million people. The unique positioning of the Wasatch Front and the surrounding geography means that the region is regularly impacted by meteorological events that impact air quality. Windblown dust from dry lake beds and anthropogenic activities (e.g., mining, oil and gas, cattle grazing), wildfire smoke from large-scale fires in the western US, and winter inversions all negatively affect air quality.

Dust transported to urban areas along the Wasatch Front from desert regions frequently affect air quality. The Great Salt Lake, Sevier Dry Lake and other playas across the eastern Great Basin are remnants of Pleistocene Lake Bonneville that serve as dust "hot spots" in the region (Fig. 1). Lake Bonneville reached a maximum depth at ~14.4 ^{14}C ka before partially draining in mega floods and finally drying to modern levels (Hart et al., 2004; Jarret and Malde, 1987; O'Connor et al., 2020; Oviatt, 2015). In August 2021, the Great Salt Lake reached a historic low mark resulting in a ~with a 44% decline in lake surface area since 1986. To the south, Sevier Dry Lake is a remnant of former Lake Gunnison that formed when Lake Bonneville separated into two basins. Sevier Dry Lake was filled with water until the mid-1800s but dried due to water diversions. The lake bed has remained dry with the exception of high snow-melt years (Oviatt, 1988). Dust is regularly transported from these and other regional playas to urban areas with an

average of 4.3-4.7 dust events a year (Steenburgh et al., 2012). Dust events are often associated with strong winds from the southwest during cold fronts or baroclinic troughs during the spring and fall (Hahnenberger and Nicoll, 2012; Nicoll et al., 2020; Steenburgh et al., 2012). Previous work identified distinct $^{87}Sr/^{86}Sr$ ratios for SDL (0.7100) and GSL (0.7150) (Carling et al., 2020).

The Wasatch Front is afflicted by winter inversions that typically occur December-February but can occur any time cold air stagnation forms. Winter inversions are meteorological events that cause cold air to stagnate in valleys below a cap of warmer air. Stagnation of air in metropolitan areas trap pollutants and form a persistent fog that is frequently observed. Air quality during inversions becomes more severe the longer the inversion lasts. Winter inversions have been the subject of much concern along the Wasatch Front, but no studies have directly measured metal concentrations in the air during inversion events (Gillies et al., 2010; Simon Wang et al., 2015; Whiteman et al., 1999; Wolyn and McKee, 1989a)

Fireworks are used in holidays and festivals year-round along the Wasatch Front. Though fireworks are illegal in most cities because of the high fire risk, they are permitted around the Independence Day (4 July), Pioneer Day (24 July), and New Year's Eve (31 December). Ba, Cu, K, Mg, and Sr salts are present in fireworks as color producers. The health implications of fireworks have been studied significantly worldwide (Seidel and Birnbaum, 2015; Singh et al., 2019; Steinhauser et al., 2008; Vecchi et al., 2008; Wilkin et al., 2007). The Utah Department of Air Quality monitors air quality during firework events using PM_{10} and $PM_{2.5}$ concentrations in the air but no studies have directly measured metal concentrations in the air during firework events along the Wasatch Front.

3. Methods

3.1 Active PM Sampling

To characterize ambient air conditions and contributions from dust events, wildfire smoke, fireworks, and urban pollution, we installed three MiniVol TAS Portable Air Samplers with $PM_{2.5}$, PM_{10} and Total Suspended Particulate (TSP) impactors at Brigham Young University in Provo, Utah (Fig. 1). $PM_{2.5}$ and PM_{10} are fine particles with an aerodynamic diameter less than 2.5 and 10 microns, respectively. Collectors were placed on the roof top of a four-story building to minimize local disturbances. Filters were collected every two weeks from May 2019 to September 2021 for a total of 163 samples (58 TSP, 50 PM_{10}, 52 $PM_{2.5}$). During the summer and fall of 2021, two MiniVol (PM2.5 and PM 10) samplers were removed from the roof and used for short term deployments near gravel pits along the Wasatch Front.

In addition to samples collected in Provo, archived filters were supplied by the Utah Department of Air Quality (UDAQ). In total, 30 filters were analyzed from August 2008 to September 2009 that were collected near Hawthorne Elementary in Salt Lake City (SLC) (Fig. 1). Filters were deployed for 24-hour periods.

To characterize the local dust signature along the Wasatch front, MiniVol air samplers were placed near gravel pits in Lehi, Utah (JNP). Air samplers were placed at other gravel pit locations but there was insufficient PM collected for analyses.

3.2 Snow Dust Sampling

To compare dust chemistry in the mountains to urban dry deposition, dust was collected from mountain snowpack in the Uinta Mountains near Trial Lake and in the Wasatch Mountains

near Alta, Utah during April 2021 (Fig. 1). We dug snow pits, identified dust layers in the snowpack, and filled a 1L FLPE bottle with dusty snow for each horizon. We identified two dust layers in the Uinta snowpack and one dust layer in the Wasatch snowpack.

3.3 Bulk Deposition Sampling

To characterize differences between active air filters and passive bulk atmospheric deposition, a separate marble collector was placed adjacent to a MiniVol air sampler at our Provo site. Bulk deposition was collected in a 50 gallon tote lined with a plastic bag and covered with an acid leached plastic screen and marbles to provide a surface for dust deposition (Reheis and Kihl, 1995). Samples were collected from February 2021 to September 2021 with a 6-week deployment period providing a total of 5 bulk atmospheric deposition samples. At the end of each sample period, the marbles and screen were rinsed with Milli-Q water before the plastic bag was removed from the tote. The resulting slurry was then transferred into acid rinsed 1L FLPE bottles. All slurry samples (snow and bulk deposition samples) were dried at 120°C until ~5mL of slurry remained. The remaining slurry was left to evaporate at room temperature to reduce risk of mineral precipitation.

3.4 Sample Analyses

All samples were analyzed for major and trace element concentrations. Filter samples were prepared for analysis following a two-step sequential acid leaching procedure. A sequential leaching process was chosen to quantify the easily leachable or "bioavailable" fraction and the residual fraction. The total concentration of each element was calculated as the sum of both leaching steps. Filters were folded to fit inside an acid-washed 50 mL centrifuge tube. We added 7 mL of 1M acetic acid (CH_3COOH) to each sample and the samples were shaken vigorously for

~24 hours using a shake table. Samples were centrifuged at 4000 rpm for 3-6 minutes before the solution was pipetted off into acid-washed 15 mL centrifuge tubes. The leaching process was then repeated with 6 mL of aqua regia (1:3 ratio of concentrated nitric acid to hydrochloric acid).

Snow dust and bulk marble samples were subjected to a four-step sequential leaching procedure. We used 4mL of 1M ammonium acetate (NH_4AcO), 1M acetic acid, 1M nitric acid (HNO_3), and 1M aqua regia to identify different mineral fractions in the dust. The ammonium acetate extracts the water-soluble fraction, acetic acid extracts the carbonate mineral fraction and water-soluble fraction when ammonium acetate was not used, the nitric acid extracts the clay and feldspar fraction, and aqua regia extracts the residual fraction though not all remaining material was completely dissolved (Naiman et al., 2000; Whiteman et al., 2014).

Sample leachates were analyzed for major and trace element concentrations using an Agilent 7500cc quadrupole inductively coupled plasma mass spectrometer (ICP-MS) with a collision cell, a double-pass spry chamber with perfluoroalkoxy (PFA) nebulizer (0.1 mL/min), a quartz torch, and platinum cones at the University of Utah. Analysis yielded concentrations for 44 elements including Ag, Al, As, B, Ba, Be, Ca, Cd, Ce, Co, Cr, Cs, Cu, Dy, Er, Eu, Fe, Gd, Ho, K, La, Li, Lu, Mg, Mn, Mo, Na, Nd, Ni, Pb, Pr, Rb, Sb, Se, Sm, Sr, Tb, Th, Tl, U, V, Y, Yb, and Zn.

The acetic acid effectively reacts with the carbonate mineral fraction of dust and soils for $^{87}Sr/^{86}Sr$ analysis (Carling et al., 2020). Samples with sufficient Sr concentration (>40 ppb Sr) were analyzed for $^{87}Sr/^{86}Sr$ ratios. All samples with sufficient mass (n = 164) were analyzed for $^{87}Sr/^{86}Sr$ ratios on the acetic acid leachate using a Thermo Scientific Neptune multicollector ICP-MS. The samples were purified inline using a Sr-FAST ion chromatographic column packed with crown ether resin (Mackey and Fernandez, 2011). Analytical precision (2σSE) of all

samples ranged from ±0.000008-0.000080. The $^{87}Sr/^{86}Sr$ ratios were corrected for mass bias using exponential law, normalizing to $^{87}Sr/^{86}Sr = 0.1194$ (Steiger and Jäger, 1977). Isobaric interferences, such as from ^{87}Rb and ^{86}Kr, were corrected simultaneously monitoring ^{85}Rb and ^{83}Kr using the corresponding invariant ratios of $^{87}Rb/^{85}Rb = 0.385706$ and $^{86}Kr/^{83}Kr = 1.502522$ (Steiger and Jäger, 1977).

3.5 Data Quality Control

To prepare for statistical analysis, some elements or samples were removed that were below detection limit or were outliers. When the element concentration value was below detection limit (<DL) the specific value was set at ½ minimum element concentration. The element Ag was consistently below DL so was not considered in statistical analysis. Total element concentrations for each sample were calculated by adding all leachate concentrations. When the dust weight collected on the filter was sufficiently small, the resulting element concentrations were either below detection limit or anomalously large compared to other samples. In either case, if <0.0001 g of dust was collected then the sample was removed from consideration. In total 13 samples were removed from further analysis and one element (Ag) was disregarded in all samples.

3.6 Data Analysis

Raw chemistry data was interpreted using time-series plots, PMF, and PCA. Time series plots were created using total concentrations by summing the concentrations in the acetic and aqua regia leachates. The software EPA PMF 5.0 was used to identify different PM factors along the Wasatch Front. Concentration data from PM_{10} filters produced the most robust results. The Base Model was run 20 times with a random seed to identify factors. We ran 100 bootstraps

using the most robust Base Model result to verify the model. Principal Component Analysis was performed using MATLAB to produce new axes of principal components (PC). PCA takes a multi-variable data set, in which each variable is an independent axis, and reorients the axis to describe the greatest amount of variation with the fewest number of dimensions. The PCA was performed on samples from the active sampler in Provo using the total element concentrations in the $PM_{2.5}$, PM_{10}, and TSP filters (n = 150).

4. Results

4.1 Concentration Time-series Show Impacts from Fireworks and Urban Pollution

Two groups of elements were identified in time-series plots. The first group was elements emitted by fireworks and the second group was elements concentrated by winter pollution. Mineral dust element concentrations (Al, Ca, Fe, Mg, U, REEs) were highest in TSP and lowest in $PM_{2.5}$, but variations from seasonality and spikes from episodic dust events were not easily identifiable in time-series.

The elements Ba, Cu, K, and Sr had peaks in concentrations around the Fourth of July in 2019, 2020, and 2021 (Fig. 2). In July 2019, K concentrations increased >1800% over the previous measured period, which was the greatest element increase. The lowest change was Cu and Sr with ~300% increase. Each year, element concentrations increased at all size fractions with the greatest increase in $PM_{2.5}$ followed by PM_{10}. This is opposite of the normal trend where TSP typically contains higher concentrations year-round. New Year's Eve was not identifiable in raw data.

Another group of elements identified are typically sourced from anthropogenic activity. The elements As, Cd, Pb, and Tl increased in concentrations during winter months in all size

fractions (Fig. 3). Of the size fractions, TSP showed the greatest increase in concentrations, while $PM_{2.5}$ showed the lowest increase. Winter pollution from these elements begins in mid-November and ends in mid-February. During this time, winter inversions are a common event that can concentrate PM in the atmosphere.

4.2 Multivariate Analysis Indicates Three Groups of Elements Dominate Chemistry

Principal Component Analysis on total element concentrations revealed 3 principal components that explained 83% of the variance (Fig. 4). PC 1 retains 63.6% of the variance and is explained by Al, Be, Ca, Co, Cs, Fe, Li, Mg, Mg, Rb, Th, U, Y, and REEs. PC 2 retains 11.3% of the variance and is explained by As, Cd, Mo, Pb, Sb, Tl, and Zn. PC 3 retains 8.1% of the variance and is explained by Ba, Cr, Cu, K, Sr, and V.

When plotting PCs in a times series, each PC shows a unique pattern (Fig. 5). Total suspended particulate size fraction is most affected by PC 1 while $PM_{2.5}$ is the least affected. Size fractions in PC 2 remain consistent with each other and over time resemble a sinusoidal curve with maximums occurring in December and minimums in June. Strong peaks exist beginning in November and can occur as late as February. In PC 3, there is no significant fractionation between particle sizes. Strong peaks in PC 3 occur around the Fourth of July in 2019 and 2020, and minor peaks around New Year's Eve 2020 and the Fourth of July 2021.

PMF on PM_{10} filters resulted in 5 factors (Fig. 6). Factor 1 explains V, Cr, and Gd. Factor 2 explains the anthropogenic elements As, Cd, Cu, Mo, Pb, Sb, Tl, and Zn. Factor 3 explains elements commonly found in silicic and evaporite minerals, Al, Be, Ca, K, Li, Mg, Rb, Sr, Th, U, Y, and REEs. Factor 4 explains the elements Ba, Cu, K, La, Mo, Sb, Se. Factor 5 explains B,

Be, Cs, Mg, Mn, Rb, Sr, and REEs. Bootstrap results show minor smearing of factors 1 and 4 (<10 misidentified factors).

4.3 Sr Isotope Ratios Show Distinct Sr Sources Over Time

Strontium isotope ratios ($^{87}Sr/^{86}Sr$) from Provo filters ranged from 0.70796 to 0.71212 between June 2019 and August 2021 (Fig. 7). $^{87}Sr/^{86}Sr$ ratios from SLC were higher with a range from 0.70945 to 0.71538. Yearly minimums for Provo and SLC occurred around the Fourth of July regardless of location or year. $^{87}Sr/^{86}Sr$ ratios in Provo show moderate seasonal variations, with highs that occurred during summer months. $^{87}Sr/^{86}Sr$ ratios in bulk deposition were similar to $^{87}Sr/^{86}Sr$ values on TSP filters (Table 1). When both active samplers and bulk samplers were deployed, the greatest difference occurred in late Spring (8 April to 20 May 2021). Bulk PM had an $^{87}Sr/^{86}Sr$ ratio of 0.71055 while TSP filters over that same time (n = 3) had an average $^{87}Sr/^{86}Sr$ ratio of 0.71115, a difference of 0.00060. $^{87}Sr/^{86}Sr$ ratios were not measured on dust from gravel mines and construction except for a PM_{10} and TSP filter from JNP (Fig. 1) on 19 September 2021. $^{87}Sr/^{86}Sr$ ratios in gravel pit dust were 0.71236 and 0.71228 on PM_{10} and TSP filters, respectively.

4.4 Sequential Leaching Results Show Bioavailability of Elements

The environmentally available fraction of the elements measured was revealed when element concentrations were compared between each leachate step (Fig. 8). TSP filters (n = 60), bulk marble samples (n = 6), and snow dust samples (n = 3) were averaged in their respective groups to identify variations. Filters were analyzed using acetic acid leachate which represents the carbonate mineral fraction and can serve as a proxy for bioavailability. On TSP filters, Na, Sr, Ca, Cd, Mg, and Zn were readily leached in the acetic acid leachate, accounting for over 70%

of element mass. Notable toxic elements with >50% abundance in the acetic acid leachate include Se, Cd, As, Tl, and Pb. In the bulk marble and snow dust samples, ammonium acetate represents the water-soluble and exchangeable fractions. In bulk samples, Na, Se, Sr, B, Mo, and K were highly water-soluble. Elements with significant portions in the carbonate mineral fraction (>30%) are Ca, Cd, Mn, Ba, Cu, Zn, and U. Snow dust was depleted in water-soluble forms of normally significant elements such as Se, Sr, B, Ca, Cd, and Mo. The silicate mineral fraction represented by nitric acid contained a higher percentage of REE's and most other elements than the filter and bulk samples.

5. Discussion

5.1 Effects Dust Events, Winter Inversions, and Fireworks on Air Quality

Exceptional events contribute PM that can greatly impact the air quality. Dust events to the Wasatch Front increase PM in the atmosphere which degrades the air quality. Particulate matter concentrations measured during dust events that we observed at the Provo site (Fig. 1) exceeded of 100 $\mu g/m^3$ for TSP and 25 $\mu g/m^3$ for $PM_{2.5}$. During a dust event on 19 September 2021, dust emitted from the JNP gravel pit reached concentrations of 192.8 $\mu g/m^3$/hour in TSP and 27 $\mu g/m^3$/hour. Increased particulate matter (PM) has been linked to increased rates of asthma, pneumonia, cardiovascular disease (Pope et al., 1990).

Winter inversions concentrate anthropogenic pollutants in the air for the duration of the inversion. Harmful elements As, Cd, Pb, and Tl increased concentrations during winter months along the Wasatch Front (Fig. 3). Concentrations of these elements increased >1000% due to winter inversions, with Pb increasing >2500% over summer baseline levels. The National Ambient Air Quality Standards (NAAQS) dictates that Pb concentrations do not exceed 0.15

$\mu g/m^3$ over a 3-month rolling average. Lead concentrations measured in TSP were 0.01 $\mu g/m^3$ over a 3-month average, well below the NAAQS standard. The highest Pb concentration (0.02 ng/m^3) was measured from 3 to 16 December 2020.

Heavy metals have been shown to concentrate in wildfire smoke and burned soils (Jovanovic et al., 2011; Sparks and Wagner, 2021). In this study, the effect of wildfires was indistinguishable from other signatures. In wildfires, the elements Cd, Cu, Pb, Sn, and Zn are enriched (Jovanovic et al., 2011; Sparks and Wagner, 2021), but the effects of winter inversions on these elements made distinguishing key chemical fingerprints impossible. For example, Cu is commonly released in PM from fires but is also greatly concentrated by winter inversions. Fires occur most frequently in July and August in the northern Hemisphere (Westerling et al., 2003), and winter inversions occur most frequently in November, December, and January (Simon Wang et al., 2015). Even though concentration of an element may increase due to wildfires in the late summer, the signal is dwarfed by the presence of winter inversions along the Wasatch Front. A more reliable method for quantifying the impact of wildfires would include analysis of organic PM alongside major and trace element chemistry (Schneider and Abbatt, 2022).

Elements typically released by fireworks into the atmosphere include Ba, Cu, K, Mg, and Sr (Vecchi et al., 2008). Element concentrations increased several times over the previous sampling period in 2019: K (4.5 times), Cu (6.5 times), Ba (5 times), and Sr (4 times). Magnesium in the fireworks samples was relatively depleted compared to dust events because mineral dust is a significant source of Mg to the Wasatch Front (Goodman et al., 2019). Strontium is also present in PM dust from playas with elevated levels in sediment from GSL (Pedone and Dickson, 2000). Copper is a common anthropogenic pollutant, but Cu

concentrations emitted during firework events were a magnitude higher than what is emitted during winter pollution.

Dust layers in snowpack represent mineral dust transported to the Uinta and Wasatch Mountains. Leachate comparisons revealed that snow dust is depleted in water-soluble and bioavailable fractions of all elements (Fig. 8). A notable exception is Na, which is typically only found in water-soluble forms. Depletion of elements in exchangeable forms indicates minerals were already substantially dissolved before sample collection in April 2021.

Numerous studies have documented the effects of COVID-19 lockdowns on air quality (Adam et al., 2021; Gautam, 2020; Jephcote et al., 2021; Ming et al., 2020; Yushin et al., 2020). Changes included reduced levels of $PM_{2.5}$, NO_2 and O_3 as well as a reduction in airborne metal concentrations. Between 4-23 March 2020, As concentration was measured at 0.1665 ng/m^3 while between 11-25 March 2021 As was measured at 0.3244 ng/m^3 in the $PM_{2.5}$. In TSP, As levels increased 0.1147 ng/m^3 (0.4521 to 0.5668 ng/m^3) between 2020 to 2021. There was little change year-on-year in the PM_{10} trace element concentrations. Similar trends were identified in Cd, Pb, and Tl.

5.2 Dust Events, Fireworks, and Local sources of Sr That Impact Sr Isotope Ratios

Between May 2019 and September 2021, we identified 10 dust events with measured $^{87}Sr/^{86}Sr$ ratios. Strontium values for these dust events in Provo ranged from 0.70994 to 0.71250 which falls between the expected values for SDL (~0.7100) and GSL (~0.7150), major dust sources in the region (Carling et al., 2020). These values line up with previous work that quantified contributions from SDL and GSL to urban areas along the Wasatch Front (Carling et al., 2020). However, by using filters that were deployed for 2-weeks rather than two months as in

previous studies, we were able to sample at a higher frequency. While most $^{87}Sr/^{86}Sr$ ratios measured were between values from SDL and GSL a few samples were below the theoretical minimum set by SDL (~0.7100) and as low as ~0.7080. It was thought that low $^{87}Sr/^{86}Sr$ values could be produced by local dust from gravel pits and construction sites. However, sampling at JNP near an active gravel mine revealed an $^{87}Sr/^{86}Sr$ value of ~0.7120. This matches work done on Sr ratios in tufa and mollusk shells in the Provo shoreline of Lake Bonneville, the primary formation targeted by gravel mine operations along the Wasatch Front (Hart et al., 2004).

Particulate matter from sources not sampled would also affect measured $^{87}Sr/^{86}Sr$ ratios. Local bedrock formations from the Carboniferous to Permian including the Great Blue Limestone and Deseret Limestone have $^{87}Sr/^{86}Sr$ ratios ~0.7080 (Blumstein et al., 2004). Oligocene/Eocene volcanic fields of the eastern Great Basin have $^{87}Sr/^{86}Sr$ ratios from 0.7070-0.7080 (Wooden et al., 1999). Particulate matter from these sources would make $^{87}Sr/^{86}Sr$ ratios in Provo PM lower than SDL.

The lowest $^{87}Sr/^{86}Sr$ ratios were recorded over weeks with holidays that included fireworks. In July 2019, four sample periods in Provo were collected, two of which were during fireworks. The first was around the Fourth of July and the second around 24 July (Pioneer Day), with two sample periods (four samples) in between. On the Fourth of July 2019, the average $^{87}Sr/^{86}Sr$ ratio between size fractions was ~0.7084. The average $^{87}Sr/^{86}Sr$ ratio between 8-22 July 2019 was 0.7097. From 22-31 July 2019 (including Pioneer Day) the $^{87}Sr/^{86}Sr$ ratio was ~0.7090. Fireworks decreased the $^{87}Sr/^{86}Sr$ ratio, but the effects were short-lived, and values normalized between events. The effect of fireworks was observed over the Fourth of July in 2009, 2019, 2020, and 2021. Fireworks were also observed around New Year's Eve 2020, and Pioneer Day 2019, and 2020. It should be noted there is no published source for $^{87}Sr/^{86}Sr$ ratios in fireworks.

5.3 Geochemical Fingerprints from PCA and PMF reveal Distinct PM Sources

Principal Component Analysis on total concentrations from active samples in Provo identified dust, winter pollution, and firework smoke in the first three PCs. PC 1, explained by elements commonly found in silicate and carbonate minerals, had the greatest variation in TSP samples, while $PM_{2.5}$ samples showed little variation over the study period. The most frequent PM size transported to urban areas along the Wasatch Front is 15.63-31.25 μm (Goodman et al., 2019) which is included in TSP, but not $PM_{2.5}$ (particulate matter <2.5 μm). PC 2 is explained by elements common in winter pollution and winter inversions. Values from PC 2 are lower during summer months and highest in winter when meteorological conditions trap pollutants in valleys. Peaks in PC 2 correlate with known winter inversion periods. PC 3 is explained by Ba, Cu, and K, which are commonly found in fireworks. Peaks in the PC 3 time series correspond to the Fourth of July and New Year's Eve. Troughs correspond to exceptionally bad winter inversions.

We successfully identified PMF fingerprints related to mineral dust, anthropogenic signatures, and a partial firework signal. Elements commonly found in silicate and evaporite minerals that form mineral dust are mostly found in Factor 3. Factor 2 is made up of anthropogenic elements that are concentrated in the atmosphere during winter inversions. The high levels of Cu and K in fireworks contributed to the abundance seen in Factor 4. The other major peak is La which is a byproduct of oil refining (Kulkarni et al., 2007). Factor 5 is notable because of a major peak in B (>70% explained). Boron is an important micronutrient for plant growth and is commonly added to fertilizers as borax or borates for agricultural use (Byers et al., 2001). Fugitive dust from agriculture would contain a mixture of fertilizers high in B compared to natural soils and mineral dust with significant REE influence shown in Factor 5.

5.4 Bioavailable Elements in Urban Areas and Mountain Snowpack

Water-soluble forms of heavy metals have implications for human and environmental health due to the ease with which they are absorbed into animals and plants. Environmentally available fractions of elements are represented in the ammonium acetate and acetic acid leachates. Ammonium acetate represents the exchangeable and water-soluble forms of elements and acetic acid represents element forms that are soluble under slightly acidic conditions present in soils (Fig. 8).

In an urban setting, over 50% of Cd and As at the Provo site was removed with the acetic acid leachate, suggesting that these elements are highly bioavailable (Fig. 8). These elements are contributed to the atmosphere mostly through manmade pollution and accumulate in the air during winter inversions. Fireworks contributed Sr, K, Ba, and Cu to the atmosphere and these elements are in forms that are more readily available in the environment (>70% of element mass was removed in the acetic acid fraction). Elements found in evaporite and carbonate minerals, including Na, Ca, and Mg, were also readily leached, with over 60% removed in the acetic acid fraction.

The bioavailable fractions of elements were lower in snowpack compared to urban settings. Nearly every element was depleted in the ammonium acetate and acetic acid fractions relative to urban samples except for Na, which mostly appears in halite from playa dust sources (Goodman et al., 2019). Depletion of water-soluble forms is likely due to partial melting of snow before sample collection was completed. Melt water in snow leached readily available elements leaving organic (HNO_3) and residual (aqua regia) fractions that aid in soil formation (Lawrence et al., 2013).

6. Conclusion

Trace elements in particulate matter collected along the Wasatch Front, Utah, USA comes from a combination of dust events, wildfire smoke, winter inversions, and fireworks. Dust from dry lake beds in the eastern Great Basin is blown to urban areas on the Wasatch Front during dust events. Dust events greatly increase the PM concentrations in the air, which is associated with respiratory health risks. Winter inversions contribute high levels of metals, including As, Cd, Pb and Tl to the atmosphere. Fireworks also contribute significant amounts of PM and metals to the air over short time periods, contributing Ba, Cu, K, and Sr. Strontium isotope ratios ($^{87}Sr/^{86}Sr$) were used to identify firework events over multiple years. The use of statistical models including PCA and PMF were successful in identifying dust, wildfire smoke, inversions, and fireworks as primary contributors of trace elements in PM across the region. Particulate matter in mountain snowpack showed signs of partial dissolution of these water-soluble elements including As, Cd, and Cu that are highly soluble (>50%). By analyzing PM collected in urban areas and snowpack, this study has implications for understanding levels of toxic elements that are suspended in the atmosphere and may contribute to poor air quality.

7. Tables

Table 1: $^{87}Sr/^{86}Sr$ ratios in Bulk deposition from marble samplers versus TSP filters

Date Range	**Bulk (6 weeks)**	**TSP (6-week average)**	**Difference**
2/26/21 – 4/8/21	0.71045	0.71056	-0.00011
4/8/21 – 5/20/21	0.71055	0.71115	-0.00060
5/20/21 – 7/1/21	0.71044	0.71035	0.00009
7/1/21 – 8/12/21	0.70929	0.70914	0.00015

8. Figures

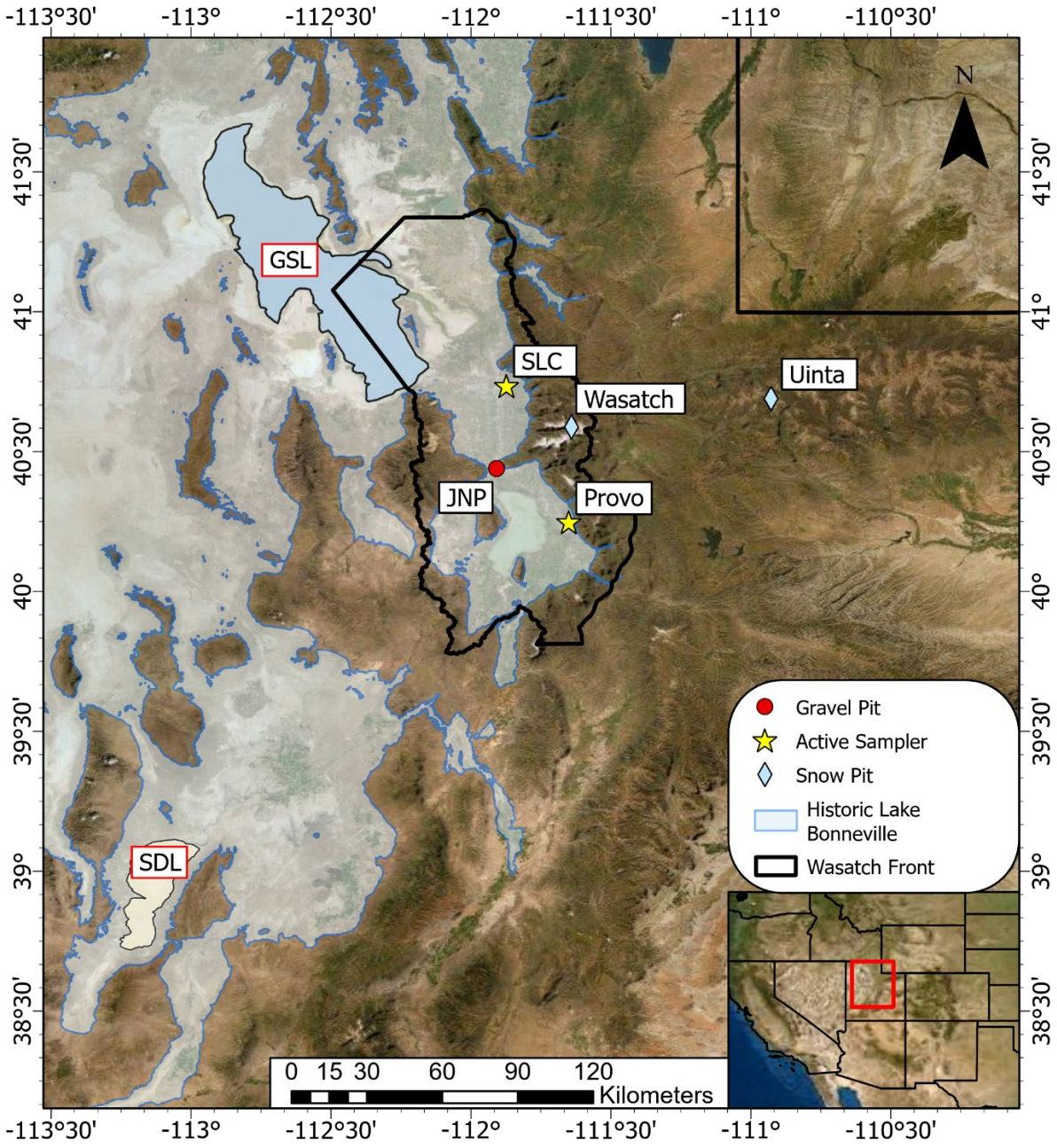

Figure 1: Dust sampling locations in Utah, USA. Active samplers were placed on roof tops at BYU campus in Provo, UT, and Hawthorne Elementary School near Salt Lake City, UT. Dust source samples were collected downwind of construction sites and gravel pits during high wind days. Snow dust samples were collected near Trial Lake in the Uinta Mountains and near Alta, Utah.

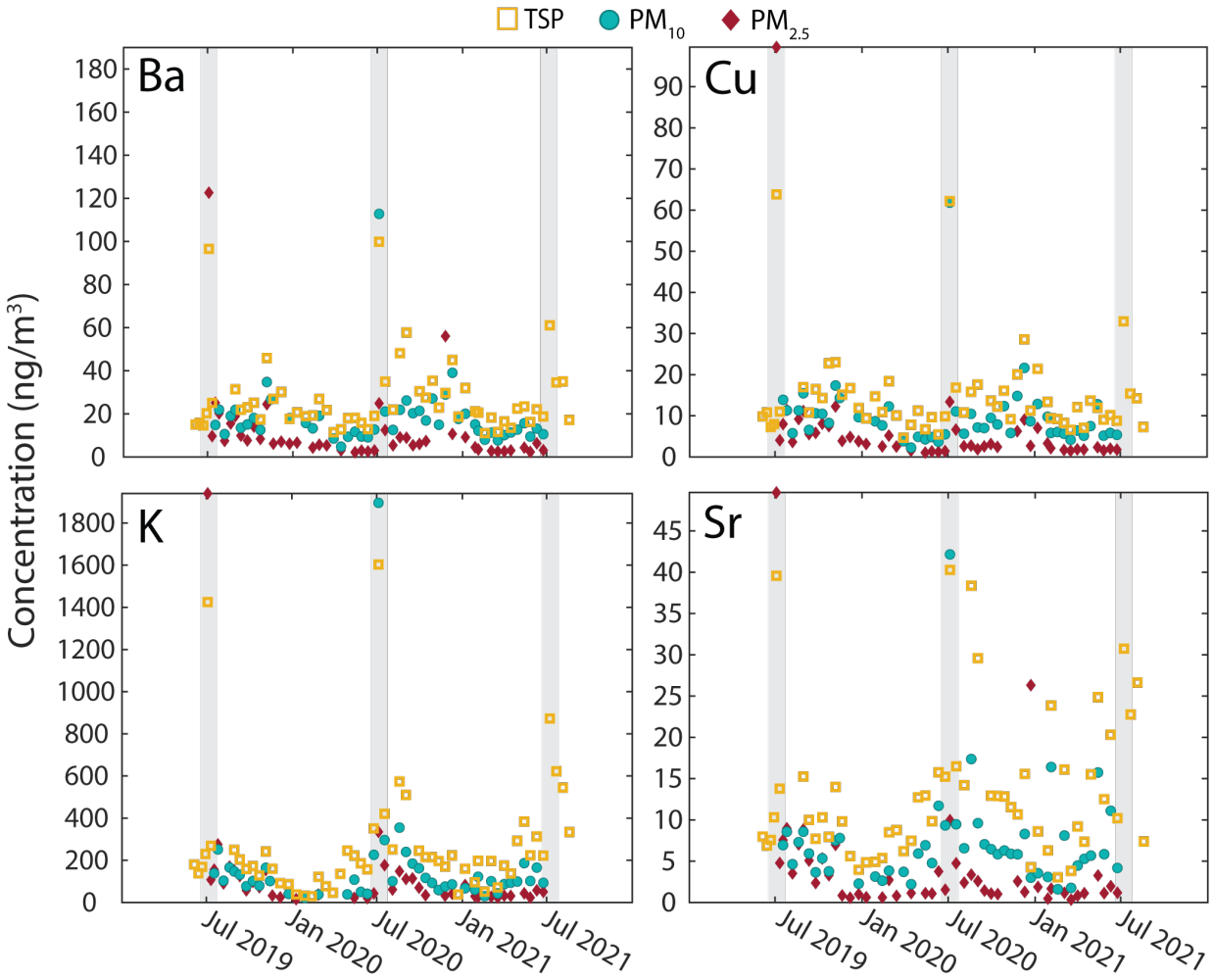

Figure 2: Total concentration of elements found in fireworks. Spikes in concentrations occur around the Fourth of July. New Years is not clearly identifiable in concentration data. Cu and Sr are commonly found in other sources of PM with Cu from other anthropogenic sources and Sr in dust.

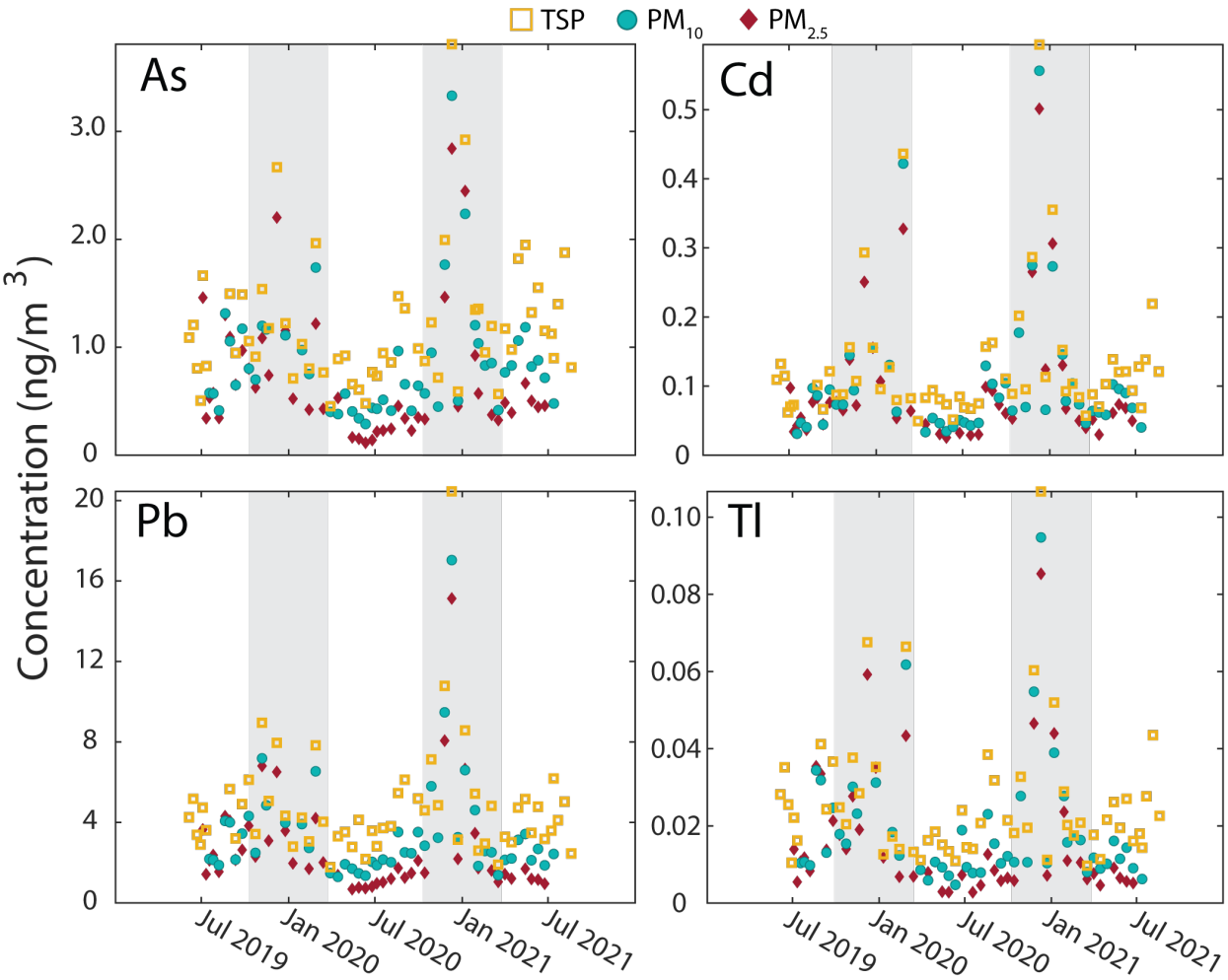

Figure 3: Total concentrations of elements that increase during winter months. Gray bars highlight from mid-November to mid-February when winter inversions typically occur.

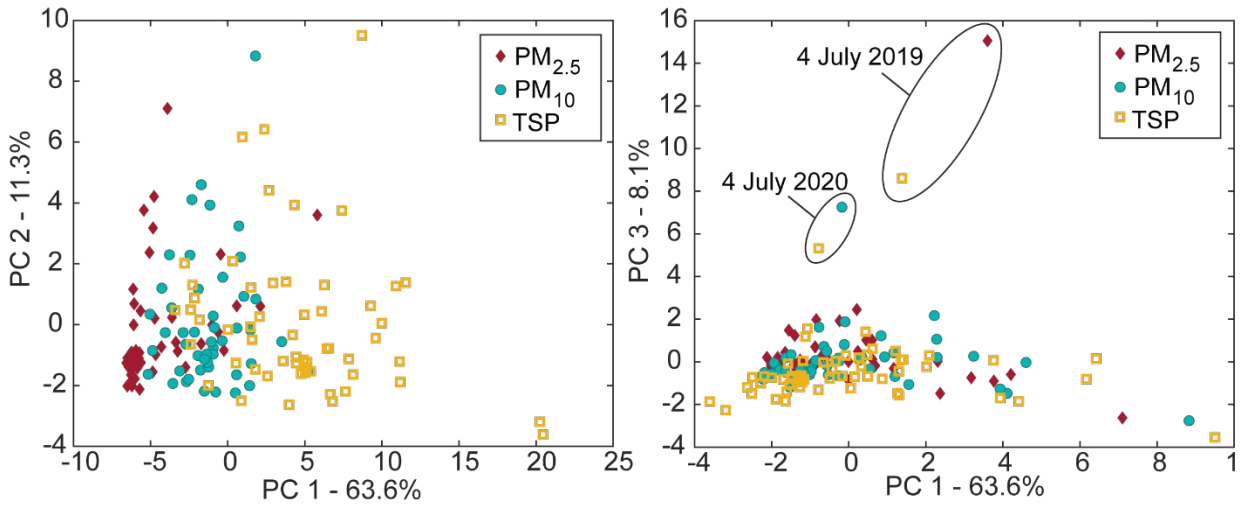

Figure 4: PCA results on all active samples from Provo. PC 1 explains 63.6% of the variance in the data. Variation in PC 1 is explained by the elements Al, Be, Co, Fe, Li, Mg, Na, Rb, Th, U, and REE's. These elements are commonly found in carbonate and silicate mineral dust. PC 2 explains 11.3% of the variance. Variation in PC 2 is explained by the elements As, Cd, Mo, Pb, Sb, Tl, and Zn. These elements are commonly found in anthropogenic pollution that is concentrated during winter months. PCA results on total concentrations from active samplers in Provo. PC 3 explains 8.1% of the variance and is explained by the elements Ba, Cr, Cu, K, Sr, and V. The elements Ba, Cu, K, and Sr are commonly found in fireworks. The Fourth of July produced the highest PC 3 values while New Year's Eve was indistinguishable from the other data.

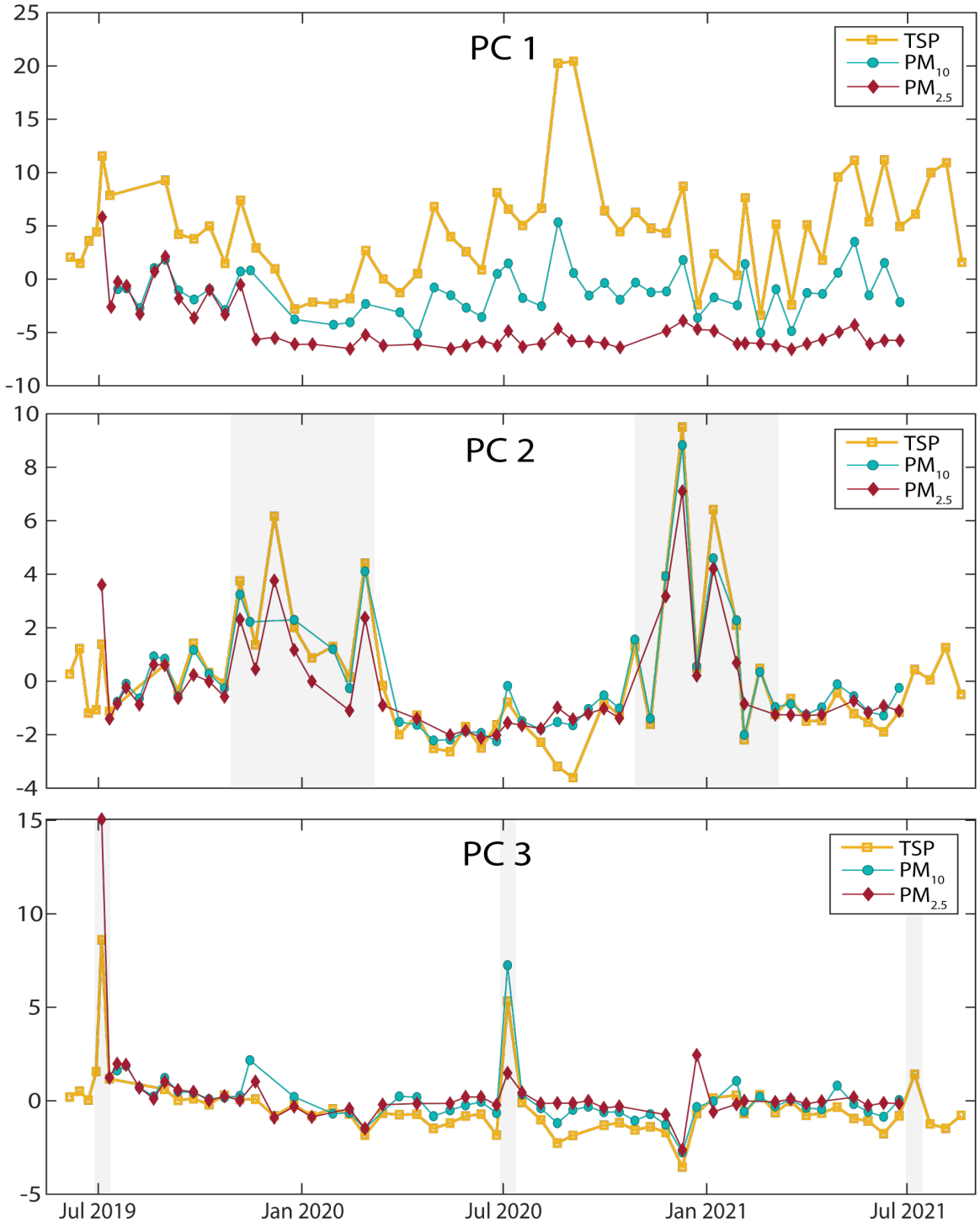

Figure 5: Time series plots of PC 1, PC 2, and PC 3. PC 1 shows the size fractions TSP is most affected by dust and dust events while $PM_{2.5}$ is not. PC 2 reflects a sinusoidal wave with peaks during winter months and troughs during summer months. Spikes in the data align with inversion events. PC 3 shows spikes during firework days including the Fourth of July and New Year's Eve

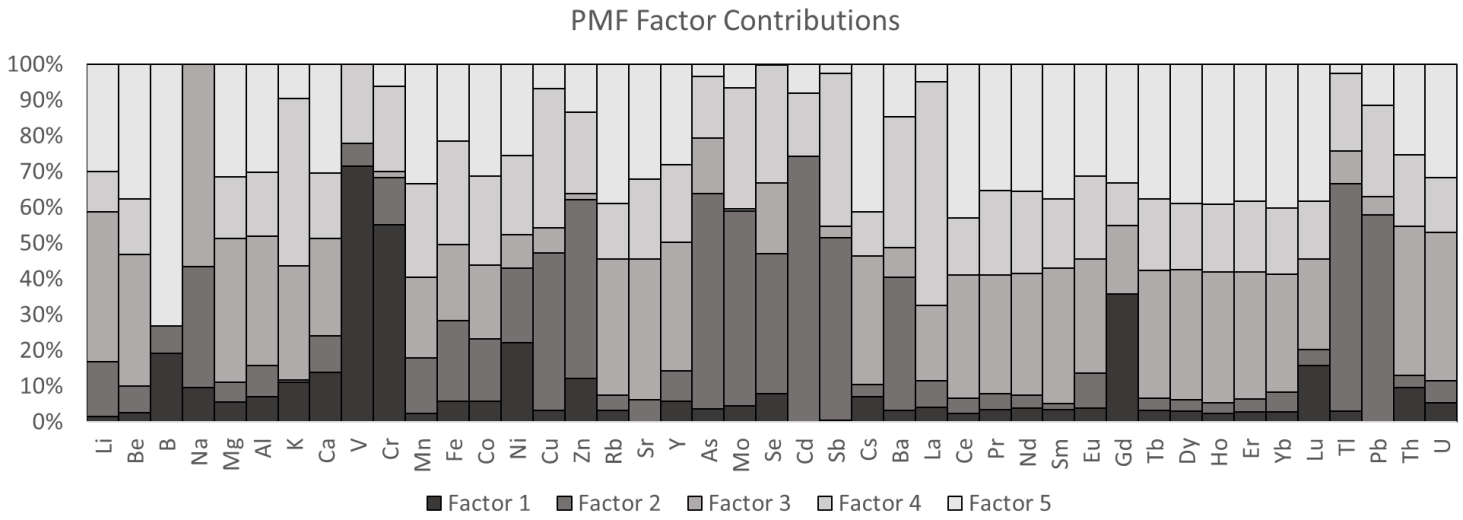

Figure 6: Percent of species present in each factor from PMF. Factor 1 is a combination of V, Cr, and Gd. Factor 2 is a combination of anthropogenically sourced elements including Cu, Zn, As, Mo, Se, Cd, Sb, Ba, Pb, and Tl. Factor 3 has elements associated with carbonate and silicate minerals including Li, Be, Na, Mg, Al, K, Ca, Rb, Sr, Th, U, and REE's. Factor 4 is combination of fireworks and other anthropogenic elements including K, Cu, and La. Factor 5 is explained by dust from local sources including B from agriculture.

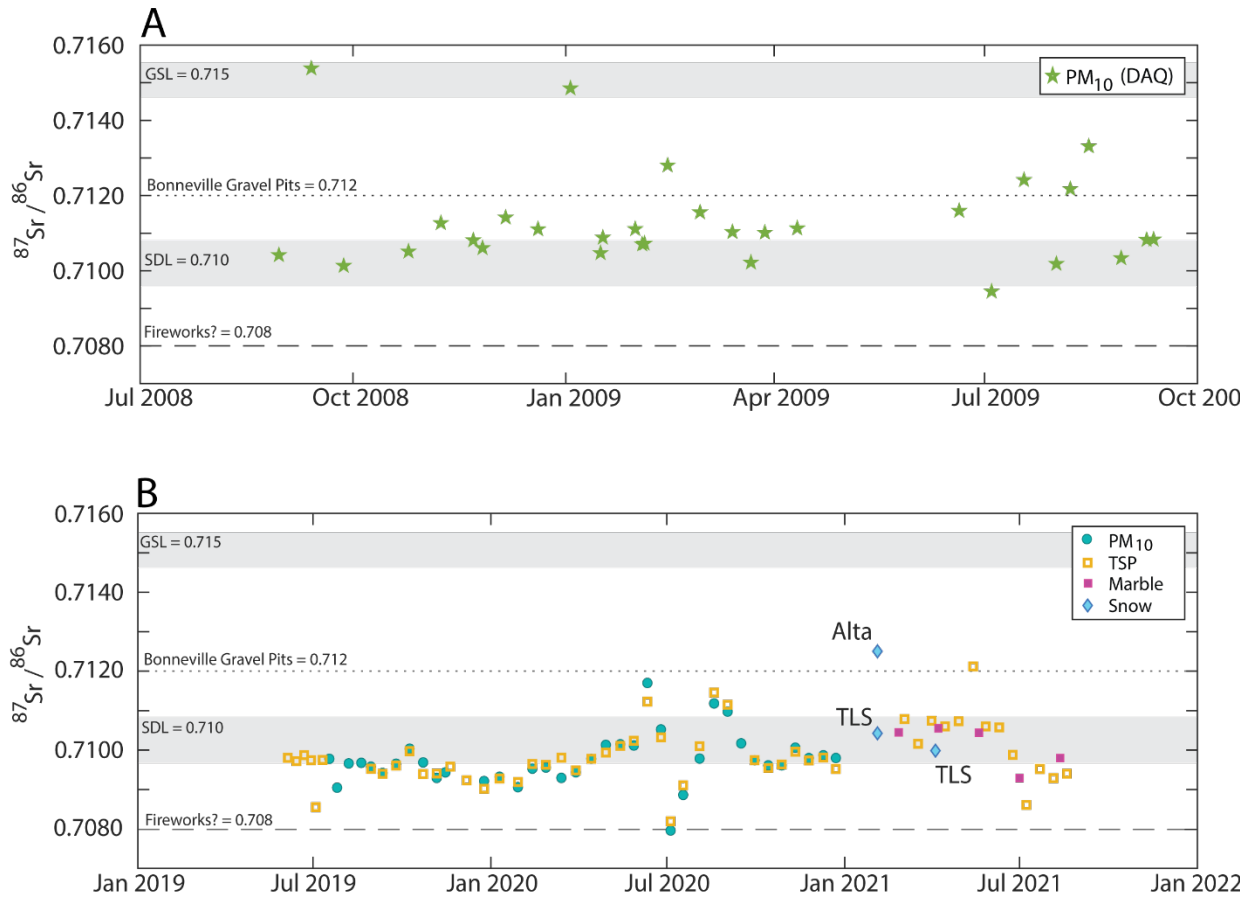

Figure 7: Sr isotope ($^{87}Sr/^{86}Sr$) ratios measured on $PM_{2.5}$, PM_{10}, and TSP filters. Sr isotope ratios were also measured for dust collected from bulk deposition on marble samplers, and snow dust horizons. Values for GSL and SDL are from Carling et al (2020). Bonneville Gravel is from Provo Shoreline deposits from Lake Bonneville. A) Sr isotope ratios on PM_{10} filters placed at Hawthorne Elementary in Salt Lake City (SLC). B) Sr isotope ratios measured on filters and bulk deposition marble samplers from Provo, UT, and snow dust horizons from the Wasatch and Uinta Mountains. Filters were in place from June 2019 through August 2021 and bulk samplers from February through September 2021. Snow dust horizons are associated with storms on 4 February and 5 April 2021.

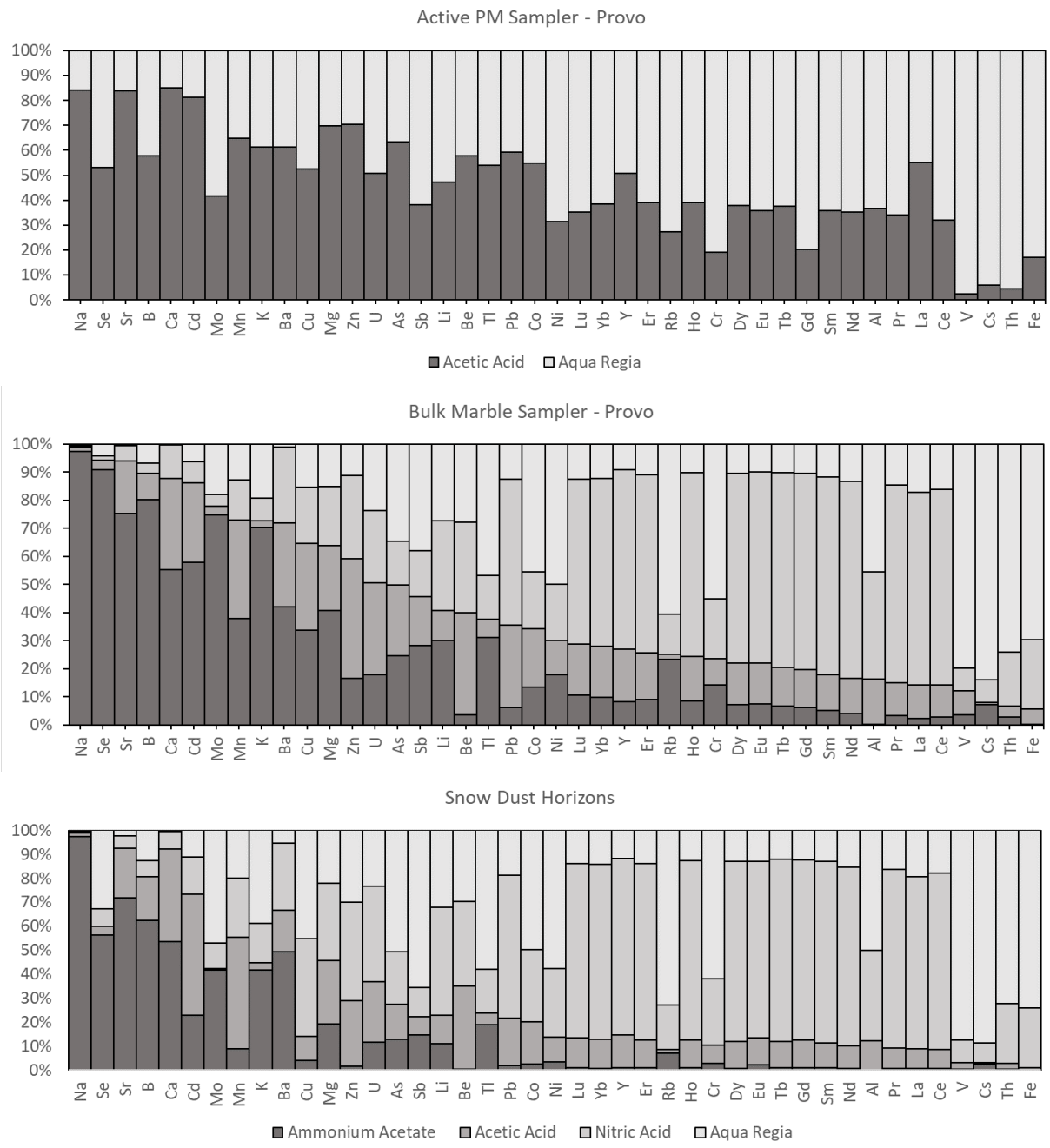

Figure 8: Results from leachate comparisons. The relative abundance of each element in the acetic acid leachate and aqua regia leachate in TSP filter samples taken in Provo(n=60). Elements in a water soluble or bioavailable form are represented in the acetic acid while insoluble forms are in the aqua regia.

9. References

Aarons, S. M., Blakowski, M. A., Aciego, S. M., Stevenson, E. I., Sims, K. W. W., Scott, S. R., and Aarons, C., 2017, Geochemical characterization of critical dust source regions in the American West: Geochimica et Cosmochimica Acta, v. 215, p. 141-161.

Adam, M. G., Tran, P. T. M., and Balasubramanian, R., 2021, Air quality changes in cities during the COVID-19 lockdown: A critical review: Atmospheric Research, v. 264, p. 105823.

Beavington, F., and Cawse, P. A., 1979, The deposition of trace elements and major nutrients in dust and rainwater in northern Nigeria: Science of The Total Environment, v. 13, no. 3, p. 263-274.

Belnap, J., and Gillette, D. A., 1998, Vulnerability of desert biological soil crusts to wind erosion: the influences of crust development, soil texture, and disturbance: Journal of Arid Environments, v. 39, no. 2, p. 133-142.

Beuck, H., Quass, U., Klemm, O., and Kuhlbusch, T. A. J., 2011, Assessment of sea salt and mineral dust contributions to PM10 in NW Germany using tracer models and positive matrix factorization: Atmospheric Environment, v. 45, no. 32, p. 5813-5821.

Blumstein, A. M., Elmore, R. D., Engel, M. H., Elliot, C., and Basu, A., 2004, Paleomagnetic dating of burial diagenesis in Mississippian carbonates, Utah: Journal of Geophysical Research: Solid Earth, v. 109, no. B4, p. n/a-n/a.

Brown, S. G., Eberly, S., Paatero, P., and Norris, G. A., 2015, Methods for estimating uncertainty in PMF solutions: Examples with ambient air and water quality data and guidance on reporting PMF results: Science of The Total Environment, v. 518-519, p. 626-635.

Byers, D. E., Mikkelsen, R. L., and Cox, F. R., 2001, GREENHOUSE EVALUATION OF FOUR BORON FERTILIZER MATERIALS: Journal of Plant Nutrition, v. 24, no. 4-5, p. 717-725.

Carling, G. T., Fernandez, D. P., and Johnson, W. P., 2012, Dust-mediated loading of trace and major elements to Wasatch Mountain snowpack: Science of The Total Environment, v. 432, p. 65-77.

Carling, G. T., Fernandez, D. P., Rey, K. A., Hale, C. A., Goodman, M. M., and Nelson, S. T., 2020, Using strontium isotopes to trace dust from a drying Great Salt Lake to adjacent urban areas and mountain snowpack: Environmental Research Letters, v. 15, no. 11, p. 114035.

Dastrup, D. B., Carling, G. T., Collins, S. A., Nelson, S. T., Fernandez, D. P., Tingey, D. G., Hahnenberger, M., and Aanderud, Z. T., 2018, Aeolian dust chemistry and bacterial communities in snow are unique to airshed locations across northern Utah, USA: Atmospheric Environment, v. 193, p. 251-261.

Gautam, S., 2020, The Influence of COVID-19 on Air Quality in India: A Boon or Inutile: Bulletin of Environmental Contamination and Toxicology, v. 104, no. 6, p. 724-726.

Gillies, R. R., Wang, S.-Y., and Booth, M. R., 2010, Atmospheric Scale Interaction on Wintertime Intermountain West Low-Level Inversions: Weather and Forecasting, v. 25, no. 4, p. 1196-1210.

Goodman, M. M., Carling, G. T., Fernandez, D. P., Rey, K. A., Hale, C. A., Bickmore, B. R., Nelson, S. T., and Munroe, J. S., 2019, Trace element chemistry of atmospheric

deposition along the Wasatch Front (Utah, USA) reflects regional playa dust and local urban aerosols: Chemical Geology, v. 530, p. 119317.
Goudie, A. S., 2009, Dust storms: Recent developments: Journal of Environmental Management, v. 90, no. 1, p. 89-94.
-, 2014, Desert dust and human health disorders: Environment International, v. 63, p. 101-113.
Grousset, F. E., and Biscaye, P. E., 2005, Tracing dust sources and transport patterns using Sr, Nd and Pb isotopes: Chemical Geology, v. 222, no. 3-4, p. 149-167.
Hahnenberger, M., and Nicoll, K., 2012, Meteorological characteristics of dust storm events in the eastern Great Basin of Utah, U.S.A.: Atmospheric Environment, v. 60, p. 601-612.
Hart, W. S., Quade, J., Madsen, D. B., Kaufman, D. S., and Oviatt, C. G., 2004, The 87Sr/86Sr ratios of lacustrine carbonates and lake-level history of the Bonneville paleolake system: Geological Society of America Bulletin, v. 116, no. 9, p. 1107.
He, C., Breuning-Madsen, H., and Awadzi, T. W., 2007, Mineralogy of dust deposited during the Harmattan season in Ghana: Geografisk Tidsskrift-Danish Journal of Geography, v. 107, no. 1, p. 9-15.
Indoitu, R., Kozhoridze, G., Batyrbaeva, M., Vitkovskaya, I., Orlovsky, N., Blumberg, D., and Orlovsky, L., 2015, Dust emission and environmental changes in the dried bottom of the Aral Sea, Volume 17: Aeolian Research.
Jarret, R. D., and Malde, H. E., 1987, Paleodischarge of the late Pleistocene Bonneveille Flood, Snake River, Idaho computed from new evidence: Geological Society of America Bulletin, v. 99, p. 127-134.
Jephcote, C., Hansell, A. L., Adams, K., and Gulliver, J., 2021, Changes in air quality during COVID-19 ‘lockdown’ in the United Kingdom: Environmental Pollution, v. 272, p. 116011.
Jovanovic, V. P. S., Ilic, M. D., Markovic, M. S., Mitic, V. D., Nikolic Mandic, S. D., and Stojanovic, G. S., 2011, Wild fire impact on copper, zinc, lead and cadmium distribution in soil and relation with abundance in selected plants of Lamiaceae family from Vidlic Mountain (Serbia): Chemosphere, v. 84, no. 11, p. 1584-1591.
Karagulian, F., Belis, C. A., Dora, C. F. C., Prüss-Ustün, A. M., Bonjour, S., Adair-Rohani, H., and Amann, M., 2015, Contributions to cities' ambient particulate matter (PM): A systematic review of local source contributions at global level: Atmospheric Environment, v. 120, p. 475-483.
Kulkarni, P., Chellam, S., and Fraser, M. P., 2007, Tracking Petroleum Refinery Emission Events Using Lanthanum and Lanthanides as Elemental Markers for PM2.5: Environmental Science & Technology, v. 41, no. 19, p. 6748-6754.
Lanno, R., Wells, J., Conder, J., Bradham, K., and Basta, N., 2004, The bioavailability of chemicals in soil for earthworms: Ecotoxicology and Environmental Safety, v. 57, no. 1, p. 39-47.
Lawrence, C. R., Reynolds, R. L., Ketterer, M. E., and Neff, J. C., 2013, Aeolian controls of soil geochemistry and weathering fluxes in high-elevation ecosystems of the Rocky Mountains, Colorado: Geochimica et Cosmochimica Acta, v. 107, p. 27-46.
Lee, E., Chan, C. K., and Paatero, P., 1999, Application of positive matrix factorization in source apportionment of particulate pollutants in Hong Kong: Atmospheric Environment, v. 33, no. 19, p. 3201-3212.
Mackey, G. N., and Fernandez, D. P., 2011, High throughput Sr isotope analysis using an automated column chemistry system: AGU Fall Meeting.

Micklin, P., 2010, The past, present, and future Aral Sea: Lakes & Reservoirs: Science, Policy and Management for Sustainable Use, v. 15, no. 3, p. 193-213.
Miller-Schulze, J. P., Shafer, M., Schauer, J. J., Heo, J., Solomon, P. A., Lantz, J., Artamonova, M., Chen, B., Imashev, S., Sverdlik, L., Carmichael, G., and DeMinter, J., 2015, Seasonal contribution of mineral dust and other major components to particulate matter at two remote sites in Central Asia: Atmospheric Environment, v. 119, p. 11-20.
Ming, W., Zhou, Z., Ai, H., Bi, H., and Zhong, Y., 2020, COVID-19 and Air Quality: Evidence from China: Emerging Markets Finance and Trade, v. 56, no. 10, p. 2422-2442.
Moreno, T., Querol, X., Alastuey, A., De La Rosa, J., Sánchez De La Campa, A. M., Minguillón, M., Pandolfi, M., González-Castanedo, Y., Monfort, E., and Gibbons, W., 2010, Variations in vanadium, nickel and lanthanoid element concentrations in urban air: Science of The Total Environment, v. 408, no. 20, p. 4569-4579.
Munroe, J. S., Norris, E. D., Carling, G. T., Beard, B. L., Satkoski, A. M., and Liu, L., 2019, Isotope fingerprinting reveals western North American sources of modern dust in the Uinta Mountains, Utah, USA: Aeolian Research, v. 38, p. 39-47.
Naiman, Z., Quade, J., and Patchett, P. J., 2000, Isotopic evidnence for eolian recycling of pedogenic carbonate and variations in carbonate dust sources throughout the southwest United States: Geochemica et Cosmochima Acta, v. 64, no. 18, p. 3099-3109.
Neff, J. C., Ballantyne, A. P., Mahowald, N. M., Conroy, J. L., Landry, C. C., Overpeck, J. T., Painter, T. H., Lawrence, C. R., and Reynolds, R. L., 2008, Increasing eolian dust deposition in the western United States linked to human activity: Nature Geoscience, p. 189-195.
Nicolás, J., Chiari, M., Crespo, J., Orellana, I. G., Lucarelli, F., Nava, S., Pastor, C., and Yubero, E., 2008, Quantification of Saharan and local dust impact in an arid Mediterranean area by the positive matrix factorization (PMF) technique: Atmospheric Environment, v. 42, no. 39, p. 8872-8882.
Nicoll, K., Hahnenberger, M., and Goldstein, H. L., 2020, 'Dust in the wind' from source-to-sink: Analysis of the 14–15 April 2015 storm in Utah: Aeolian Research, v. 46, p. 100532.
O'Connor, J. E., Baker, V. R., Waitt, R. B., Smith, L. N., Cannon, C. M., George, D. L., and Denlinger, R. P., 2020, The Missoula and Bonneville floods—A review of ice-age megafloods in the Columbia River basin: Earth-Science Reviews, v. 208, p. 103181.
Oviatt, C. G., 1988, Late Pleistocene and Holocene lake fluctuations in the Sevier Lake basin, Utah, USA: Journal of Paleolimnology, v. 1, no. 1, p. 9-21.
-, 2015, Chronology of Lake Bonneville, 30,000 to 10,000 yr B.P: Quaternary Science Reviews, v. 110, p. 166-171.
Painter, T. H., Barrett, A. P., Landry, C. C., Neff, J. C., Cassidy, M. P., Lawrence, C. R., Mcbride, K. E., and Farmer, G. L., 2007, Impact of disturbed desert soils on duration of mountain snow cover: Geophysical Research Letters, v. 34, no. 12.
Painter, T. H., Deems, J. S., and Belnap, J., 2010, Response of Colorado River runoff to dust radiative forcing in snow, Volume 107: PNAS, p. 17125-17130.
Pedone, V. A., and Dickson, J. A. D., 2000, Replacement of Aragonite by Quasi-Rhombohedral Dolomite in a Late Pleistocene Tufa Mound, Great Salt Lake, Utah, U.S.A.: Journal of Sedimentary Research, v. 70, no. 5, p. 1152-1159.

Pope, A. C., Dockery, D. W., Spengler, J. D., and Raizenne, M. E., 1990, Respiratory Health and PM10 Pollution: A Daily Time Series Analysis, American Review of Respiratory Diseases.

Pope, C. A., Hill, R. W., and Villegas, G. M., 1999, Particulate air pollution and daily mortality on Utah's Wasatch Front.: Environmental Health Perspectives, v. 107, no. 7, p. 567-573.

Prospero, J. M., 2002, Environmental characterization of global sources of atmospheric soil dust identified with the NIMBUS 7 Total Ozone Mapping Spectrometer (TOMS) absorbing aerosol product: Reviews of Geophysics, v. 40, no. 1.

Reheis, M. C., and Kihl, R., 1995, Dust deposition in southern Nevada and California, 1984–1989: Relations to climate, source area, and source lithology: Journal of Geophysical Research, v. 100, no. D5, p. 8893.

Reynolds, R. L., Yount, J. C., Reheis, M., Goldstein, H., Chavez, P., Fulton, R., Whitney, J., Fuller, C., and Forester, R. M., 2007, Dust emission from wet and dry playas in the Mojave Desert, USA: Earth Surface Processes and Landforms, v. 32, no. 12, p. 1811-1827.

Schneider, S. R., and Abbatt, J. P. D., 2022, Wildfire atmospheric chemistry: climate and air quality impacts: Trends in Chemistry, v. 4, no. 4, p. 255-257.

Seidel, D. J., and Birnbaum, A. N., 2015, Effects of Independence Day fireworks on atmospheric concentrations of fine particulate matter in the United States: Atmospheric Environment, v. 115, p. 192-198.

Simon Wang, S.-Y., Hipps, L. E., Chung, O.-Y., Gillies, R. R., and Martin, R., 2015, Long-Term Winter Inversion Properties in a Mountain Valley of the Western United States and Implications on Air Quality: Journal of Applied Meteorology and Climatology, v. 54, no. 12, p. 2339-2352.

Singh, A., Pant, P., and Pope, F. D., 2019, Air quality during and after festivals: Aerosol concentrations, composition and health effects: Atmospheric Research, v. 227, p. 220-232.

Skiles, S. M., Mallia, D. V., Hallar, A. G., Lin, J. C., Lambert, A., Petersen, R., and Clark, S., 2018, Implications of a shrinking Great Salt Lake for dust on snow deposition in the Wasatch Mountains, UT, as informed by a source to sink case study from the 13–14 April 2017 dust event: Environmental Research Letters, v. 13, no. 12, p. 124031.

Sparks, T. L., and Wagner, J., 2021, Composition of particulate matter during a wildfire smoke episode in an urban area: Aerosol Science and Technology, v. 55, no. 6, p. 734-747.

Steenburgh, W. J., Massey, J. D., and Painter, T. H., 2012, Episodic Dust Events of Utah’s Wasatch Front and Adjoining Region: Journal of Applied Meteorology and Climatology, v. 51, no. 9, p. 1654-1669.

Steiger, R. H., and Jäger, E., 1977, Subcommission on geochronology: Convention on the use of decay constants in geo- and cosmochronology: Earth and Planetary Science Letters, v. 36, no. 3, p. 359-362.

Steinhauser, G., Sterba, J. H., Foster, M., Grass, F., and Bichler, M., 2008, Heavy metals from pyrotechnics in New Years Eve snow: Atmospheric Environment, v. 42, no. 37, p. 8616-8622.

Sudheer, A. K., and Rengarajan, R., 2012, Atmospheric Mineral Dust and Trace Metals over Urban Environment in Western India during Winter: Aerosol and Air Quality Research, v. 12, no. 5, p. 923-933.

Tao, J., Ho, K.-F., Chen, L., Zhu, L., Han, J., and Xu, Z., 2009, Effect of chemical composition of PM2.5 on visibility in Guangzhou, China, 2007 spring: Particuology, v. 7, no. 1, p. 68-75.

Vecchi, R., Bernardoni, V., Cricchio, D., D'Alessandro, A., Fermo, P., Lucarelli, F., Nava, S., Piazzalunga, A., and Valli, G., 2008, The impact of fireworks on airborne particles: Atmospheric Environment, v. 42, no. 6, p. 1121-1132.

Wang, J., Guo, P., Li, X., Zhu, J., Reinert, T., Heitmann, J., Spemann, D., Vogt, J., Flagmeyer, R.-H., and Butz, T., 2000, Source Identification of Lead Pollution in the Atmosphere of Shanghai City by Analyzing Single Aerosol Particles (SAP): Environmental Science & Technology, v. 34, no. 10, p. 1900-1905.

Westerling, A. L., Gershunov, A., Brown, T. J., Cayan, D. R., and Dettinger, M. D., 2003, Climate and Wildfire in the Western United States: Bulletin of the American Meteorological Society, v. 84, no. 5, p. 595-604.

Whiteman, C. D., Bian, X., and Zhong, S., 1999, Wintertime Evolution of the Temperature Inversion in the Colorado Plateau Basin: Journal of Applied Meteorology, v. 38, no. 8, p. 1103-1117.

Whiteman, C. D., Hoch, S. W., Horel, J. D., and Charland, A., 2014, Relationship between particulate air pollution and meteorological variables in Utah's Salt Lake Valley: Atmospheric Environment, v. 94, p. 742-753.

Wilkin, R. T., Fine, D. D., and Burnett, N. G., 2007, Perchlorate Behavior in a Municipal Lake Following Fireworks Displays: Environmental Science & Technology, v. 41, no. 11, p. 3966-3971.

Wolyn, P. G., and McKee, T. B., 1989a, Deep stable layers in the intermountain western United States, Volume 117, p. 461-472.

Wolyn, P. G., and McKee, T. B., 1989b, Deep Stable Layers in the Intermountain Western United States: Monthly Weather Review, v. 117, no. 3, p. 461-472.

Wooden, J. L., Kistler, R. W., and Tosdal, R. M., 1999, Strontium, lead, and oxygen isotopic data for granitoid and volcanic rocks from the northern Great Basin and Sierra Nevada, California, Nevada and Utah, 99-569.

Wurtsbaugh, W. A., Miller, C., Null, S. E., Derose, R. J., Wilcock, P., Hahnenberger, M., Howe, F., and Moore, J., 2017, Decline of the world's saline lakes: Nature Geoscience, v. 10, no. 11, p. 816-821.

Yushin, N., Chaligava, O., Zinicovscaia, I., Vergel, K., and Grozdov, D., 2020, Mosses as Bioindicators of Heavy Metal Air Pollution in the Lockdown Period Adopted to Cope with the COVID-19 Pandemic: Atmosphere, v. 11, no. 11, p. 1194.

Zhang, J., 1994, Atmospheric Wet Deposition of Nutrient Elements: Correlation with Harmful Biological Blooms in Northwest Pacific Coastal Zones: Ambio, v. 23, p. 464-468.